FY8904 Assignment 3

Filip Sund

Spring 2019

Abstract

Abstract

Introduction

NB: I seem to have mistaken ζ in the assignment text for ξ, so let's just define $\xi = \zeta$ and $\xi_0 = \zeta_0$ for convenience, since replacing the ξ's everywhere at this late stage would be hard. This has no effect on the results.

Theory

The periodic surface Rayleigh equation

We will solve numerically the *periodic surface Rayleigh equation*

$$\sum_{\boldsymbol{K}'_\parallel} \hat{I}\Big(-\alpha_0\big(K'_\parallel,\omega\big)\big|\boldsymbol{K}_\parallel - \boldsymbol{K}'_\parallel\Big) M\big(\boldsymbol{K}_\parallel\big|\boldsymbol{K}'_\parallel\big) r\big(\boldsymbol{K}'_\parallel\big|\boldsymbol{k}_\parallel\big) = -\hat{I}\Big(\alpha_0\big(k_\parallel,\omega\big)\big|\boldsymbol{K}_\parallel - \boldsymbol{k}_\parallel\Big) N\big(\boldsymbol{K}_\parallel\big|\boldsymbol{k}_\parallel\big), \tag{1}$$

or

$$\sum_{\boldsymbol{K}'_\parallel} \hat{I}\Big(-\alpha_0\big(K'_\parallel,\omega\big)\big|\boldsymbol{G}_\parallel - \boldsymbol{G}'_\parallel\Big) M\big(\boldsymbol{K}_\parallel\big|\boldsymbol{K}'_\parallel\big) r\big(\boldsymbol{K}'_\parallel\big|\boldsymbol{k}_\parallel\big) = -\hat{I}\Big(\alpha_0\big(k_\parallel,\omega\big)\big|\boldsymbol{G}_\parallel\Big) N\big(\boldsymbol{K}_\parallel\big|\boldsymbol{k}_\parallel\big), \tag{2}$$

where the lateral wave vectors $\boldsymbol{K}_\parallel$ and $\boldsymbol{K}_\parallel$ are defined as

$$\boldsymbol{K}_\parallel = \boldsymbol{k}_\parallel + \boldsymbol{G}_\parallel \qquad\qquad \boldsymbol{K}'_\parallel = \boldsymbol{k}_\parallel + \boldsymbol{G}'_\parallel, \tag{3}$$

and $\boldsymbol{G}_\parallel$ are the lattice sites of the reciprocal lattice of the doubly periodic surface profile $\xi(\boldsymbol{x})$, given by

$$\boldsymbol{G}_\parallel(\boldsymbol{h}) = h_1\boldsymbol{b}_1 + h_2\boldsymbol{b}_2, \qquad h_i \in \mathbb{Z}. \tag{4}$$

We will use a square lattice with translation vectors $\boldsymbol{a}_1 = a\hat{\boldsymbol{x}}_1$ and $\boldsymbol{a}_2 = a\hat{\boldsymbol{x}}_2$ which means that the reciprocal lattice vectors are $\boldsymbol{b}_1 = (2\pi/a)\hat{\boldsymbol{x}}_1$ and $\boldsymbol{b} = (2\pi/a)\hat{\boldsymbol{x}}_2$, and

$$\boldsymbol{G}_\parallel(\boldsymbol{h}) = h_1\frac{2\pi}{a}\hat{\boldsymbol{x}}_1 + h_2\frac{2\pi}{a}\hat{\boldsymbol{x}}_2, \qquad h_i \in \mathbb{Z}. \tag{5}$$

The wave vector $\boldsymbol{k}$ represents the incident wave, and is written in the form

$$\boldsymbol{k} = \boldsymbol{k}_\parallel \pm \alpha_0(k_\parallel,\omega)\hat{\boldsymbol{x}}_3 \tag{6}$$

with

$$\alpha_0(k_\parallel,\omega) = \begin{cases} \sqrt{\frac{\omega^2}{c^2} - k_\parallel^2} & k_\parallel^2 < \frac{\omega^2}{c^2} \\ i\sqrt{k_\parallel^2 - \frac{\omega^2}{c^2}} & k_\parallel^2 \geq \frac{\omega^2}{c^2} \end{cases}. \tag{7}$$

The wavelength of the incident beam is denoted by λ, and is related to the angular frequency ω via $\omega/c = 2\pi/\lambda$. From geometry considerations it can be shown that

$$\boldsymbol{k}_\parallel = \frac{\omega}{c}\sin\theta_0\big(\cos\phi_0, \sin\phi_0, 0\big). \tag{8}$$

The set of solutions $\big\{r\big(\boldsymbol{K}'_\parallel\big|\boldsymbol{k}_\parallel\big)\big\}$ of Eq. (1) describes the reflection of an incident scalar wave of lateral wave vector $_\parallel$ that is scattered by a periodic surface $\xi(\boldsymbol{x}_\parallel)$ into reflected waves characterized by the wave vector $\boldsymbol{K}'_\parallel$.

The $\hat{I}$-integrals are defined in the next section.

To be able to solve Eq. (1) we limit the values of

$$\boldsymbol{K}'_{\parallel}(\boldsymbol{h}) = \boldsymbol{k} + \boldsymbol{G}'_{\parallel}(\boldsymbol{h}) \tag{9}$$

by limiting the components of $\boldsymbol{h} = (h_1, h_2)$ to

$$h_i \in [-H, H] \quad (h_i \in \mathbb{Z}), \tag{10}$$

where H is a positive integer. We then have a finite set of $N = n^2 = (2H+1)^2$ unknown scattering amplitudes $r(\boldsymbol{K}'_{\parallel}|\boldsymbol{k}_{\parallel})$. We then let $\boldsymbol{K}_{\parallel}$ take the same values as $\boldsymbol{K}'_{\parallel}$, which gives us N different variants of Eq. (1). We can then express Eq. (1) as a linear system of N equations and N unknowns, $\boldsymbol{A}\boldsymbol{x} = \boldsymbol{b}$, where

$$\boldsymbol{A} = \begin{pmatrix} A_{1,1} & A_{1,2} & \dots & A_{1,N} \\ A_{2,1} & A_{2,2} & \dots & A_{2,N} \\ \vdots & \vdots & \ddots & \vdots \\ A_{N,1} & A_{N,2} & \dots & A_{N,N} \end{pmatrix} \tag{11}$$

where $A_{i,j}$ is the pre-factor before r in the sum in Eq. (1),

$$A_{i,j} = \hat{I}\Big(-\alpha_0\big(K'^{j}_{\parallel}, \omega\big)\big|\boldsymbol{K}^{i}_{\parallel} - \boldsymbol{K}'^{j}_{\parallel}\Big) M\big(\boldsymbol{K}^{i}_{\parallel}\big|\boldsymbol{K}'^{j}_{\parallel}\big), \tag{12}$$

and

$$\boldsymbol{K}^{i}_{\parallel} = \boldsymbol{K}_{\parallel}(\boldsymbol{h}_i) \tag{13}$$

$$\boldsymbol{K}'^{j}_{\parallel} = \boldsymbol{K}'_{\parallel}(\boldsymbol{h}_j) \tag{14}$$

Further we have

$$\boldsymbol{x} = \begin{pmatrix} r\Big(\boldsymbol{K}'^{1}_{\parallel}|\boldsymbol{k}_{\parallel}\Big) \\ r\Big(\boldsymbol{K}'^{2}_{\parallel}|\boldsymbol{k}_{\parallel}\Big) \\ \dots \\ r\Big(\boldsymbol{K}'^{N-1}_{\parallel}|\boldsymbol{k}_{\parallel}\Big) \\ r\Big(\boldsymbol{K}'^{N}_{\parallel}|\boldsymbol{k}_{\parallel}\Big) \end{pmatrix} \tag{15}$$

and

$$\{\boldsymbol{h}_i\} = \boldsymbol{h}_1, \boldsymbol{h}_2, \dots, \boldsymbol{h}_n = \begin{matrix} (h_1,h_1)\,, & (h_1,h_2)\,, & \dots & (h_1,h_{n-1})\,, & (h_1,h_n)\,, \\ (h_2,h_1)\,, & (h_2,h_2)\,, & \dots & (h_2,h_{n-1})\,, & (h_2,h_n)\,, \\ \vdots & \vdots & \ddots & \vdots & \vdots \\ (h_{n-1},h_1)\,, & (h_{n-1},h_2)\,, & \dots & (h_{n-1},h_{n-1})\,, & (h_{n-1},h_n)\,, \\ (h_n,h_1)\,, & (h_n,h_2)\,, & \dots & (h_n,h_{n-1})\,, & (h_n,h_n)\,. \end{matrix}$$

($\{\boldsymbol{h}_i\}$ is not not a matrix, but is represented in a matrix form above to more easily make the connection to the matrix in Eq. (11)). In practice this is implemented as

$$\boldsymbol{h}_i = (h_j, h_k) \;\text{ where }\; j = i \mathbin{/\!\!/} n \;\text{ and }\; k = i \bmod n, \tag{16}$$

where $/\!\!/$ is integer division and mod is the *modulo* operator. This allows us to loop over the linear index i in the code.

The $\hat{I}$-integral

To evaluate Eq. (1) we need to solve the $\hat{I}$-integral

$$\hat{I}(\gamma|\boldsymbol{G}_{\parallel}) = \frac{1}{a_c}\int_{a_c} \mathrm{d}^2 x_{\parallel} \exp\big(-i\boldsymbol{G}_{\parallel}\cdot\boldsymbol{x}_{\parallel}\big)\exp\big[-i\gamma\xi(\boldsymbol{x}_{\parallel})\big]. \tag{17}$$

We write a periodic surface profile as

$$\xi(\boldsymbol{x}_{\parallel}) = \sum_{\boldsymbol{\ell}} S\big(\boldsymbol{x}_{\parallel} - \boldsymbol{x}_{\parallel}(\boldsymbol{\ell})\big), \tag{18}$$

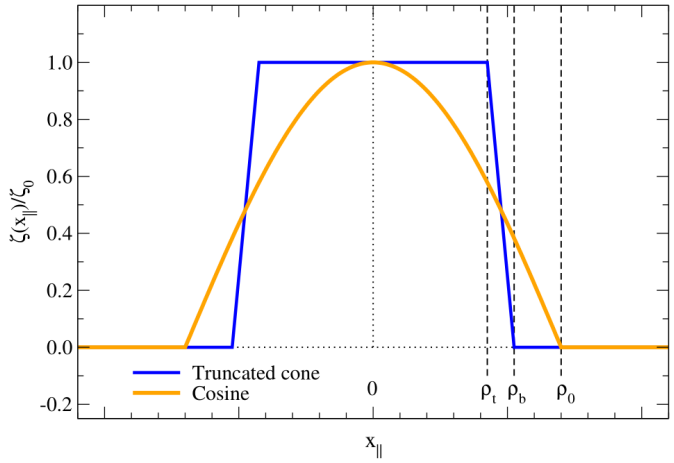

Figure 1: The truncated cone and truncated cosine forms assumed for the surface profile in the modelling. The parameters ρ_0, ρ_t and ρ_b are indicated with dashed vertical lines.

where $\{\boldsymbol{x}_\parallel(\boldsymbol{\ell})\}$ are the translation vectors of a two-dimensional Bravais lattice expressed by

$$\boldsymbol{x}_\parallel(\boldsymbol{\ell}) = l_1\boldsymbol{a}_1 + l_2\boldsymbol{a}_2. \tag{19}$$

We will use three different forms of the surface profile $\xi(\boldsymbol{x}_\parallel)$, namely the *doubly periodic cosine*

$$S(\boldsymbol{x}_\parallel) = \frac{\xi_0}{2}\left[\cos\left(\frac{2\pi x_1}{a}\right) + \cos\left(\frac{2\pi x_2}{a}\right)\right], \tag{20}$$

with amplitude ξ_0; the *truncated cone*

$$S(\boldsymbol{x}_\parallel) = \begin{cases} \xi_0 & 0 \le x_\parallel < \rho_t \\ \xi_0 \frac{\rho_b - x_\parallel}{\rho_b - \rho_t} & \rho_t \le x_\parallel < \rho_b \\ 0 & \rho_b \le x_\parallel \end{cases} \tag{21}$$

with parameters ρ_b and ρ_t governing the shape of the cone (see Fig. 1 for an illustration); and finally the *truncated cosine*

$$S(\boldsymbol{x}_\parallel) = \begin{cases} \xi_0 \cos\left(\frac{\pi x_\parallel}{2\rho_0}\right) & 0 < x_\parallel < \rho_0 \\ 0 & x_\parallel > \rho_0 \end{cases}, \tag{22}$$

with ρ_0 governing the truncation (see Fig. 1 for an illustration).

For a *doubly periodic cosine profile* of period a and amplitude ξ_0 we can calculate the $\hat{I}$-integral in closed form as [1]

$$\hat{I}\big(\gamma|\boldsymbol{G}_\parallel(\boldsymbol{h})\big) = (-i)^{h_1}\mathrm{J}_{h_1}\left(\frac{\gamma\xi_0}{2}\right)(-i)^{h_2}\mathrm{J}_{h_2}\left(\frac{\gamma\xi_0}{2}\right), \tag{23}$$

where $\mathrm{J}_n(\cdot)$ is the Bessel function of first kind and order n. The Bessel functions are evaluated via the `SciPy` function `scipy.special.jv` with the argument `order=n`.

For a truncated cone surface profile it can be shown that [1]

$$\hat{I}\big(\gamma|\boldsymbol{G}_\parallel(\boldsymbol{h})\big) = \delta_{\boldsymbol{G}_\parallel,\boldsymbol{0}} + 2\pi\frac{\rho_t^2}{a^2}\Big[\exp\left(-i\gamma\xi_0\right)\Big]\frac{J_1\big(G_\parallel\rho_t\big)}{G_\parallel\rho_t} \tag{24}$$

$$+ 2\pi\frac{\rho_b - \rho_t}{a^2}\sum_{n=1}^{\infty}\frac{(-i\gamma\xi_0)^n}{n!}\int_0^1 \mathrm{d}u_\parallel\left[\rho_b - (\rho_b - \rho_t)u_\parallel\right]J_0\Big(G_\parallel\left[\rho_b - (\rho_b - \rho_t)u_\parallel\right]\Big)u_\parallel^n, \tag{25}$$

where δ is the Kronecker-delta, and a change of variable has been performed

$$u_\parallel = \frac{\rho_b - x_\parallel}{\rho_b - \rho_t}. \tag{26}$$

Finally, for a truncated cosine surface profile we have [1]

$$\hat{I}\big(\gamma|\boldsymbol{G}_\parallel(\boldsymbol{h})\big) = \delta_{\boldsymbol{G}_\parallel,\boldsymbol{0}} + \frac{2\pi}{a^2}\sum_{n=1}^{\infty}\frac{(-i\gamma)^n}{n!}\int_0^{\rho_0} \mathrm{d}x_\parallel x_\parallel J_0\big(G_\parallel x_\parallel\big)\xi^n(x_\parallel) \tag{27}$$

The integrals in Eqs. (25) and (27) were evaluated numerically using the `numpy` function `numpy.trapz` with 100 evaluations. Enough terms were included in the sum for it to converge to within 1 % (typically 5-10 terms were needed, limited to max 20 terms). Tests at more evaluations of the integral and lower convergence limits in the sum showed no improvement in terms of energy conservation, probably due do the term $1/n!$.

Nondimensionalizing

We will be using the wavelength as the length scale when numerically solving the equations, replacing all lengths x with $x' = x/\lambda$.

Results and discussion

In Fig. 2 is a plot of the quantity $\mathcal{U}$ related to energy conservation, as function of the surface profile amplitude ξ_0/λ. It can be seen that the energy conservation diverges for $\xi_0/\lambda > 0.22$ for $a/\lambda = 0.5$ and for $\xi_0/\lambda > 1.0$ for $a/\lambda = 3.5$.

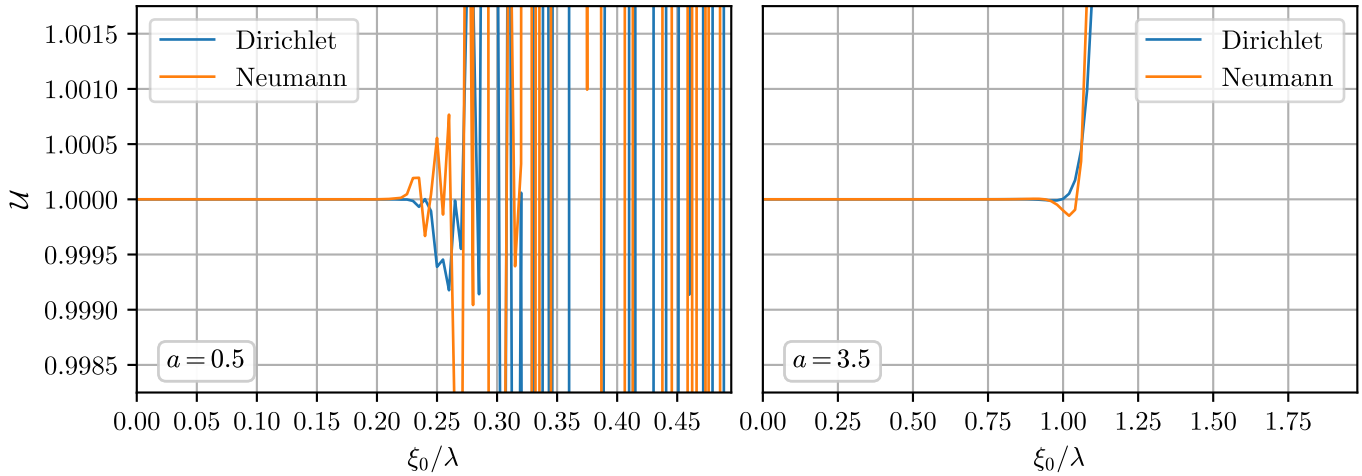

Figure 2: Plot of $\mathcal{U}$ as function of the surface profile amplitude ξ_0 for the doubly periodic cosine surface, for normal incidence $\boldsymbol{k}_\parallel = 0$. In the left plot we have used $a/\lambda = 0.5$ and in the right $a/\lambda = 3.5$. The results for both Dirichlet and Neumann surfaces are shown. A value of $H = 9$ was used in all computations. (NB: The x-limits are not the same).

Reproductions of Fig. 1, 2 and 4 in [1] are shown in Figs. 3 to 5.

How do I physically interpret Fig. 4?

Diffraction efficiencies

In figure Fig. 6 the diffraction efficiencies

$$e_m(\theta_0) = e(\boldsymbol{k}_\parallel + \boldsymbol{G}_\parallel(m)|\boldsymbol{k}_\parallel) \tag{28}$$

are show for $a/\lambda = 3.5$ and $\xi_0/\lambda = 0.05$. Here we have used

$$\boldsymbol{k}_\parallel = \frac{\omega}{c}\sin\theta_0\hat{\boldsymbol{x}}_1, \qquad \boldsymbol{G}_\parallel(k) = m\frac{2\pi}{a}\hat{\boldsymbol{x}}_1 \qquad m \in \mathbb{Z}. \tag{29}$$

(meaning $\phi_0 = 0$ and $\boldsymbol{G}_\parallel = \boldsymbol{G}_\parallel(h_1, h_2 = 0)$.)

For $a/\lambda = 0.5$ the only open/propagating diffractive channels (when $|\boldsymbol{K}_\parallel(m)| < \omega/c$) are with $m = 0$, since

$$\frac{\omega}{c} > |\boldsymbol{K}_\parallel(m)| = |\boldsymbol{k}_\parallel + \boldsymbol{G}_\parallel(m)| = \left|\frac{\omega}{c}\sin\theta_0\hat{\boldsymbol{x}}_1 + m\frac{2\pi}{0.5\lambda}\hat{\boldsymbol{x}}_1\right| = \left|\frac{\omega}{c}\sin\theta_0\hat{\boldsymbol{x}}_1 + 2m\frac{\omega}{c}\hat{\boldsymbol{x}}_1\right|$$
$$= \sqrt{\frac{\omega^2}{c^2}\sin^2\theta_0 + m^2\frac{4\pi^2}{0.5^2}} = \sqrt{\frac{\omega^2}{c^2}\sin^2\theta_0 + 4m^2\frac{\omega^2}{c^2}} = \frac{\omega}{c}\sqrt{\sin^2\theta_0 + 4m^2}$$

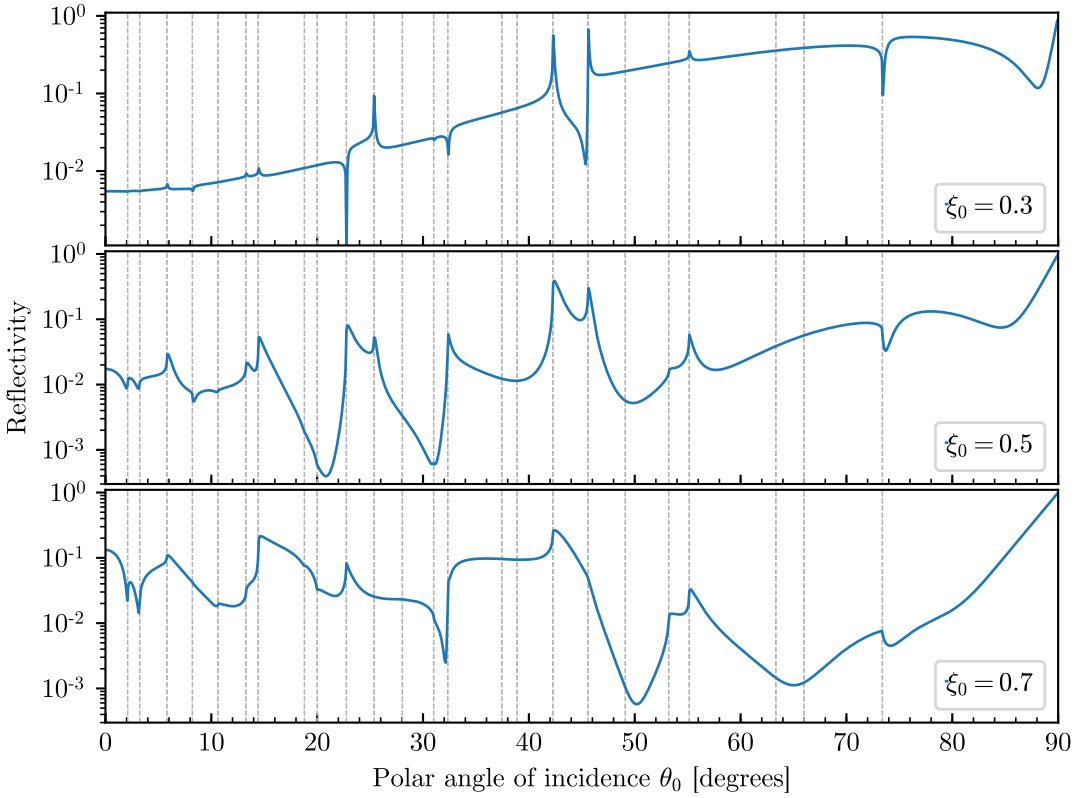

Figure 3: Reproduction of Fig. 1 in [1]. Reflectivity of a doubly-periodic cosine Neumann surface as function of the polar angle of incidence θ_0 for the azimuthal angle of incidence $\phi_0 = 0$. The doubly-periodic cosine grating had a period $a/\lambda = 3.5$ and amplitudes $\xi_0/\lambda = 0.3$ (top), $\xi_0/\lambda = 0.5$ (center) and $\xi_0/\lambda = 0.7$ (bottom), as noted in the plots. The vertical dashed lines indicate the positions of the Rayleigh anomalies predicted by Eq. (46) in [1]. The polar angles of incidence θ_0 were evaluated in 3600 steps of $\Delta\theta_0 = 0.025^\circ$ and a value of $H = 9$ was used (see Eqs. (9) and (10)).

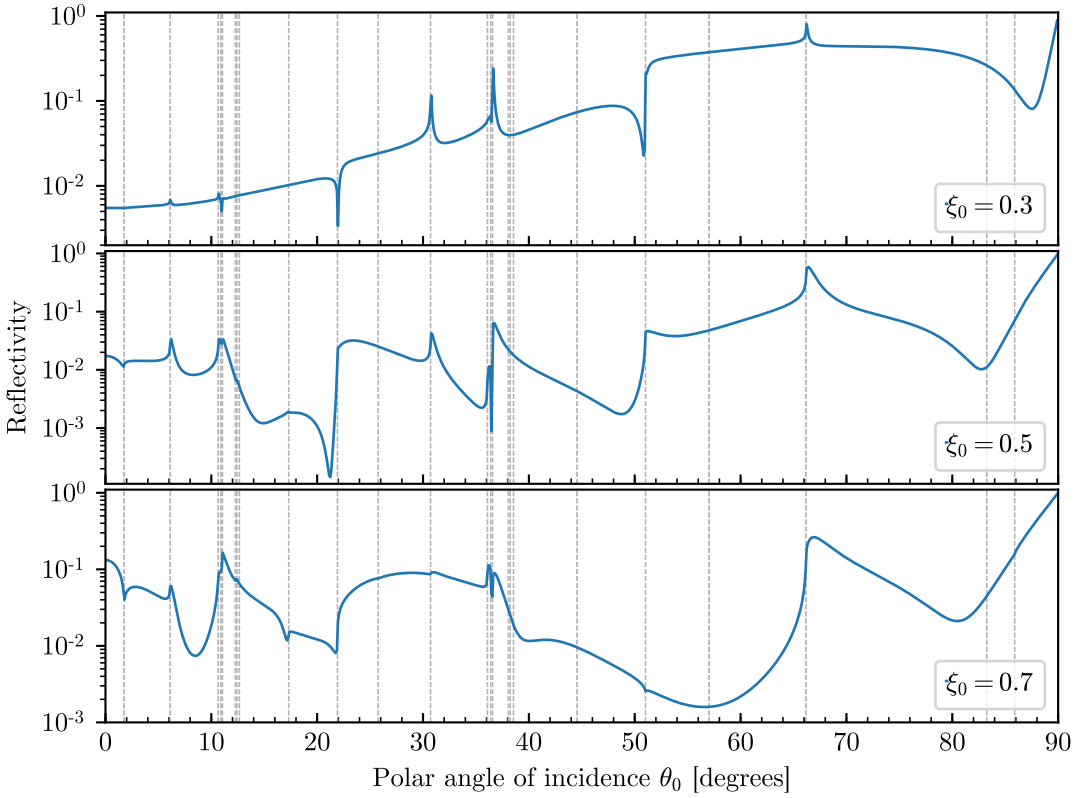

Figure 4: Reproduction of Fig. 2 in [1]. The same as Fig. 3, but for azimuthal angle of incidence $\phi_0 = 45^\circ$.

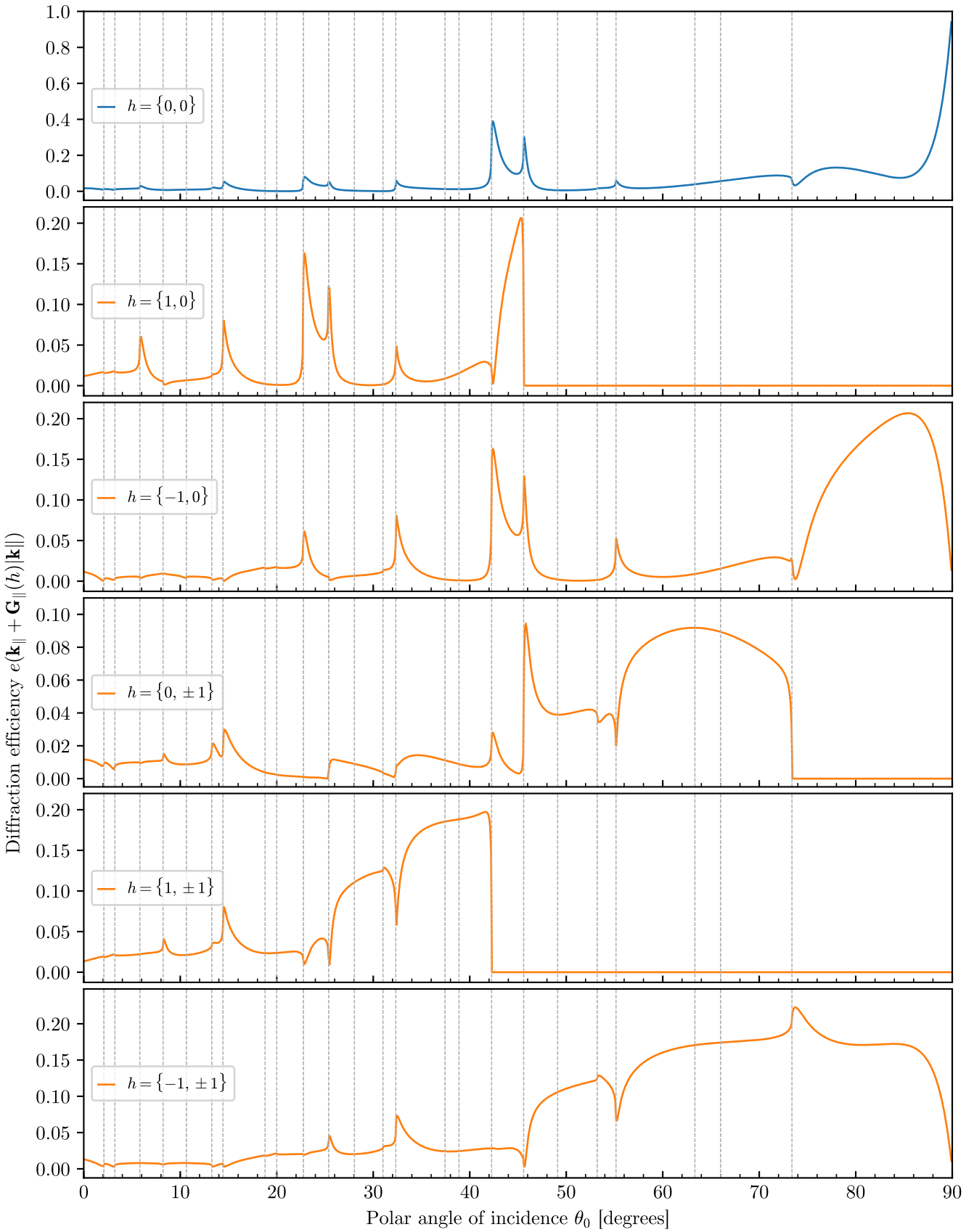

Figure 5: Reproduction of Fig. 4 in [1]. Diffraction efficiencies $e(\boldsymbol{k}_\parallel + \boldsymbol{G}_\parallel(h)|\boldsymbol{k}_\parallel)$, for values of h given in each panel, as function of the polar angle of incidence θ_0 for the azimuthal angle of incidence $\phi_0 = 0°$. The doubly-periodic Neumann surface had a period $a/\lambda = 3.5$ and amplitude $\xi_0/\lambda = 0.5$. The scan over angles θ_0 were performed in steps of $\Delta\theta_0 = 0.025°$, and a value $H = 9$ was used. **NB:** The top plot is not the same as in [1], but I think [1] by a mistake has used the data for $\xi_0/\lambda = 0.3$ instead of $\xi_0/\lambda = 0.5$ in the top plot.

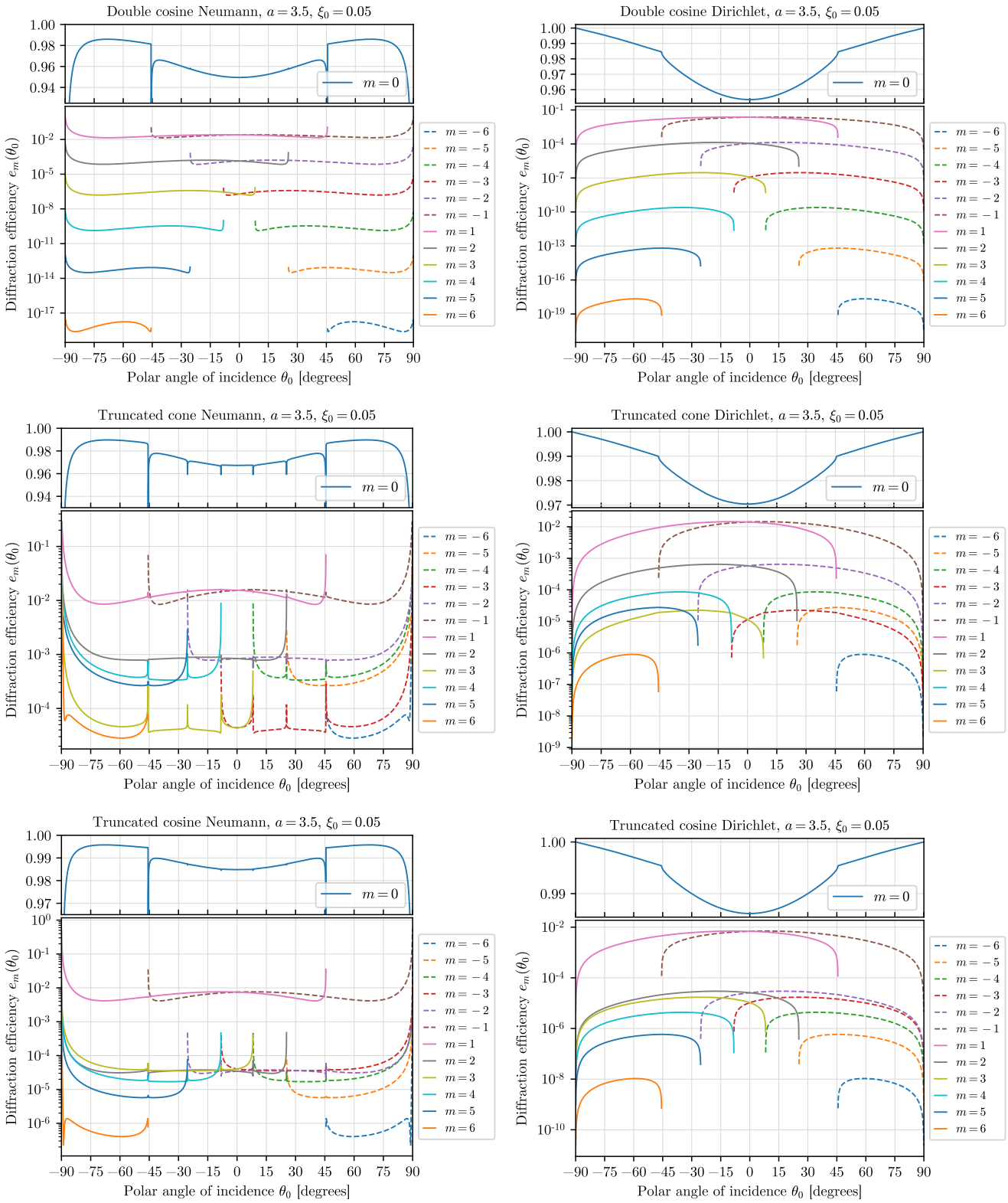

Figure 6: Diffraction efficiencies e_m for all open/propagating diffractive channels as function of the polar angle of incidence θ_0 and azimuthal angle of incidence $\phi_0 = 0$, for double cosine, truncated cone and truncated cosine surfaces with period $a/\lambda = 3.5$ and amplitude $\xi_0 = 0.05$, using both Neumann (left) and Dirichlet (right) boundary conditions. The top quarter in each figure shows $m = 0$, and the lower three quarters show the other m's with a logarithmic y-scale. For the truncated cone and cosine profiles we used $\rho_0 = (a/2) \cdot 0.8$, $\rho_b = (a/2) \cdot 0.8$ and $\rho_t = 0.8 \cdot \rho_b$. The scan over angles θ_0 were performed in steps of $\Delta\theta_0 = 0.025°$, and a value $H = 9$ was used.

and $4m^2 > 1$ for all m except $m = 0$.

For all surfaces with period $a/\lambda = 0.5$ and amplitude $\xi_0/\lambda = 0.7$ the value of $\mathcal{U}$ was within $2 \cdot 10^{-6}$ of 1 for the double cosine surface, within $3 \cdot 10^{-12}$ for the truncated cone, and within $4 \cdot 10^{-10}$ for the truncated cosine, for all angles of incidence θ_0 and both Neumann and Dirichlet boundary conditions. Since the energy conservation sum goes over $\boldsymbol{G}\|$ for which $|\boldsymbol{k}_\| + \boldsymbol{G}_\|(m)| < \omega/c$, this sum only contains one term ($m = 0$, as shown in the previous paragraph). This means that the diffraction efficiency $e_m(\theta_0)$ and energy conservation $\mathcal{U}(\theta_0)$ take on the same value. Since diffraction efficiencies are basically all ~ 1 for all angles for these surfaces we don't show any plots of that.

Interpret the diffraction efficiency results

In Fig. 7 some details from *Fig.* 6 are highlighted, specifically the results for $m = 0$, with direct comparisons between the results using Neumann and Dirichlet for each surface profile. say something smart here

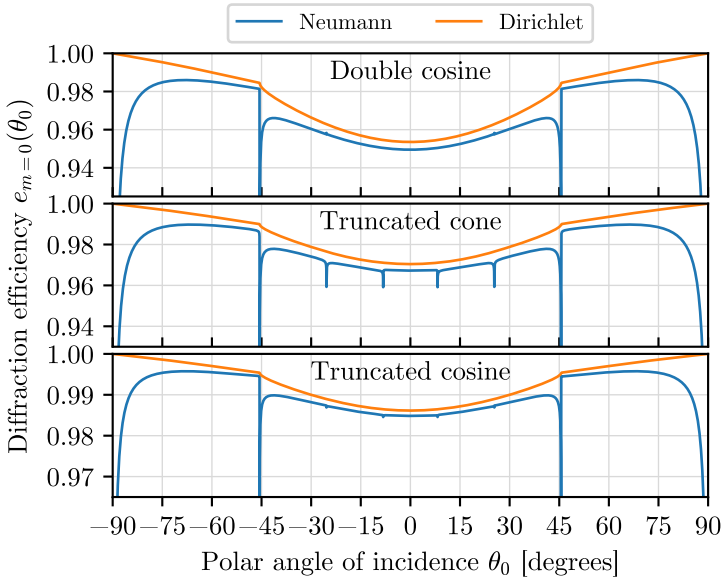

Figure 7: The same as for Fig. 6, but only showing the results $m = 0$.

In Fig. 8 plots of the quanity $\mathcal{U}$ is shown for the three surface profiles, with $a/\lambda = 3.5$ and $\xi_0 = 0.05$. The value of $\mathcal{U}$ was found to be within 1.005 for all surfaces with Neumann boundary conditions, and within 1.0006 for all surfaces with Dirichlet boundary conditions. In Fig. 8 we see that the largest deviations from for the Neumann surfaces are concentrated around $\theta_0 = \pm 90°$ and $\theta_0 = \pm 45°$.

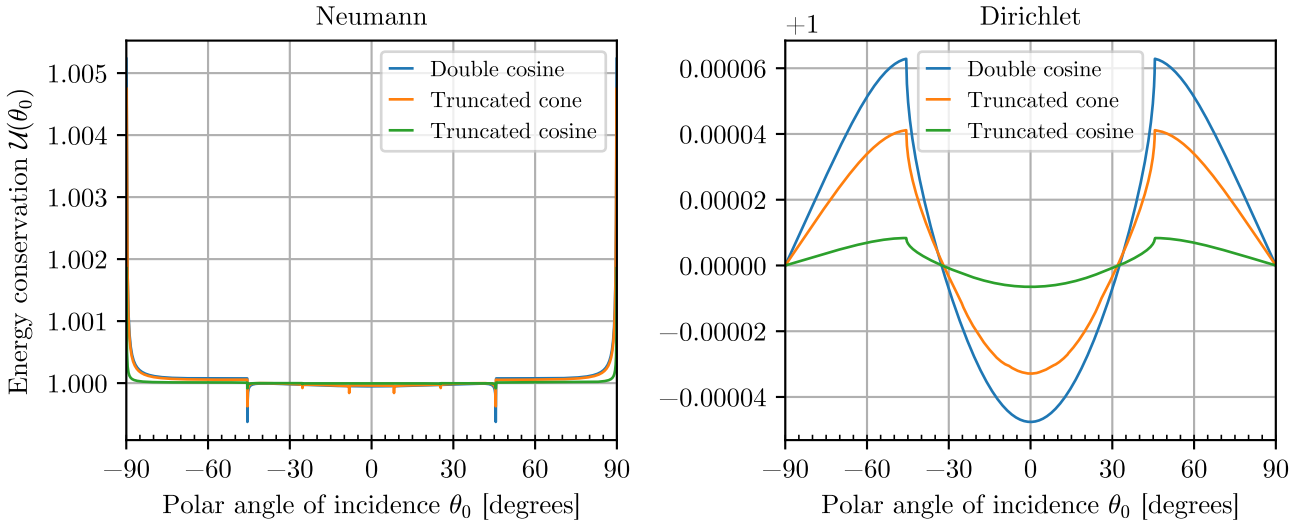

Figure 8: Plots of the energy conservation quantity $\mathcal{U}$ as function of angle of incidence θ_0 for the simulations shown in Fig. 5. (NB: Note the "+1" at the top of the y-axes, indicating that 1 should be added to the y-values.)

Other surface profiles

If the surface profile $S(\boldsymbol{x}_\parallel)$ inside a unit cell had not been available analytically as for the ones shown here, but only numerically, we would have to evaluate the $\hat{I}$-integral in Eq. (17) numerically. write something smarter here

Conclusion

- We modelled scattering of scalar waves from doubly-periodic surfaces by solving the Scrhödinger equation via the Rayleigh hypothesis.
- We found signs that the Rayleigh hypothesis breaks down around $\xi_0/\lambda > 0.22$ with a doubly periodic cosine surface with period $a/\lambda = 0.5$, and for $\xi_0/\lambda > 1.0$ when the period was $a/\lambda = 3.5$.

References

[1] A. A. Maradudin, V. Pérez-Chávez, A. Jędrzejewski, and I. Simonsen. "Features in the diffraction of a scalar plane wave from doubly-periodic Dirichlet and Neumann surfaces". In: *Low Temperature Physics* 44.7 (2018), pp. 733–743.